BIBO Stability of an Adaptive Time-Frequency Iterative Learning Control with Application to Microscale Robotic Deposition

Douglas A. Bristow and Andrew G. Alleyne, *Senior Member, IEEE*
Department of Mechanical and Industrial Engineering
University of Illinois at Urbana-Champaign
Urbana, IL 61801

***Abstract*—Microscale robotic deposition (μ-RD) is an emerging solid free-form manufacturing technique for construction of parts with microscale feature sizes. Part quality in this process is directly related to the robot tracking performance. In this paper an adaptive Iterative Learning Control algorithm using a time-varying Q-filter is presented for robust high performance tracking control of the μ-RD robot. Using a switched systems analysis, the existence of a minimum dwell time for BIBO stability is demonstrated. Experimental results show the ability of the adaptive algorithm to stably improve performance over the initial fixed filter. The recent development of multi-ink valves allows construction of parts with multiple materials interlaced throughout and a sample two-ink manufactured part is presented.**

I. Introduction

Microscale robotic deposition (μ-RD) [1] is a solid free-from manufacturing technique based on Robocasting [2]. In this technique, a robot is used to position a nozzle in 3-D space and, as the nozzle is moved over the work area, ink is extruded through the nozzle to build the desired part. The ink is usually a thixotropic ceramic-based gel [3] that exhibits fluid-like behavior under high shear when it is forced through the nozzle, but quickly regains elastic strength when shear is removed after exiting the nozzle. This behavior allows the ink to span over open gaps and to support high aspect ratio features. The μ-RD is intended to construct parts with features sizes on the microscale (0.1 μm – 100 μm), but total part sizes that may span several centimeters in length.

Figure 1 shows a picture of the μ-RD machine. The positioning system is a standard "H-drive" layout with linear motors for the X and Y axes and a rotary motor driven ballscrew for the Z axis motion. The X and Y axes are equipped with 1 μm resolution optical encoders and the Z axis uses a 0.1 μm resolution optical encoder. The ink extrusion process is controlled by an electronic pressure regulator.

This work was supported by NSF DMI-0140466 and an NSF Graduate Research Fellowship.

D. A. Bristow is a Ph.D. student at the University of Illinois at Urbana-Champaign, Urbana, IL 61801 USA (e-mail: dbristow@uiuc.edu).

A. G. Alleyne is a Professor at the University of Illinois at Urbana-Champaign, Urbana, IL 61801 USA (phone: 217-244-9993; fax: 217-244-6534; e-mail: alleyne@uiuc.edu).

Using a newly designed valve [4] shown in Figure 2, the process can switch between multiple inks to quickly and easily build prototype parts composed of multiple materials. Because errors in the robot positioning directly transfer to errors in the part, it is imperative that the robot track the desired reference with accuracy on the order of microns. It is the robot position control which will be the focus of this paper.

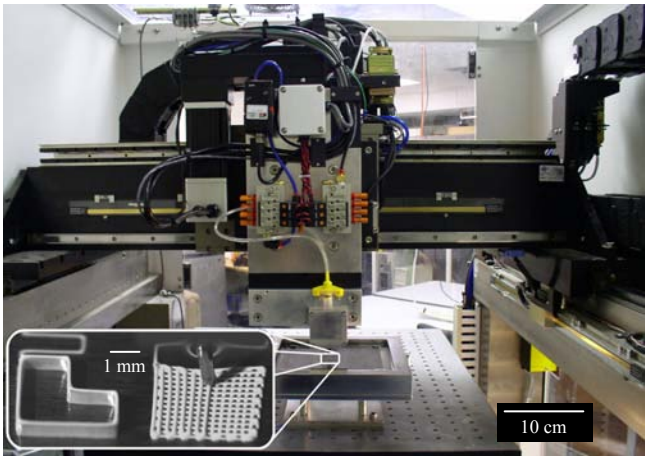

Fig. 1. Microscale robotic deposition system

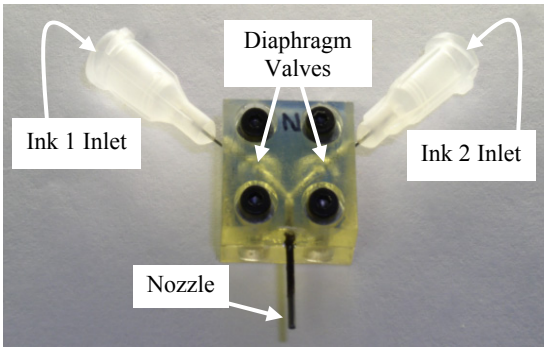

Fig. 2. Two-ink valve for multi-material part construction.

In [1], SISO dynamic models for the X, Y, and Z axes were obtained. Feedback controllers were designed to stabilize each axis and to provide a base level of tracking performance. For the μ-RD process, motions are small and errors of 10-20 μm are relatively large. In this operating regime, disturbances such as friction dominate. Friction compensation on this length scale requires very high gain feedback which creates issues with noise and excessive hardware wear. However, the target parts often exhibit a

high degree of periodicity. In this case, the Iterative Learning Control (ILC) strategy can be efficiently combined with the existing feedback controller to improve transient tracking performance [5,6]. ILC is a learning strategy that applies a feedforward signal to the system to improve performance on repeated trajectories. The feedforward signal is modified offline, after each trial, from the error signal of previous iterations. This process underlies the notion of iteratively learning from previous performance, though in fact ILC can be viewed equivalently as iteration domain feedback.

It has been demonstrated in [7,8] that the feedforward ILC signal can filtered with a time-varying Q-filter to provide an enhanced level of robustness with minimal impact on converged performance. In [7] an adaptive algorithm was designed to generate an appropriate time-varying Q-filter online. The notion of iteration-scale separation was introduced in that work to justify stability of the algorithm. In this paper a rigorous switched systems analysis is used to prove BIBO stability of the adaptive algorithm if updates occur slower than some minimum dwell time.

The rest of this paper is organized as follows. Section II presents the adaptive Q-filter ILC control algorithm. In Section III a BIBO stability proof of the adaptive algorithm is presented. Tracking results and a two-ink manufactured part are presented in Section IV. Finally, conclusions are discussed in Section V.

II. Adaptive Time-Varying Q-filtered ILC Controller

Let the discrete-time dynamics of a SISO system be described by

$$y(k) = P(q)u(k-1) + d(k)\,, \tag{1}$$

where P is a rational, stable transfer function with zero relative degree, y is the output, u is the control input, and q is the forward time shift operator defined as $qf(k) = f(k+1)$. If P is strictly proper with relative degree $m>0$, then P can be made proper by further shifting the time index of u by $-m$. The combined effects of any disturbances, initial conditions, and other inputs on the system are contained in $d(k)$. Moreover, let the desired output of the system over $k \in [1, N]$ be given by $y_d(k)$. The ILC problem is to find a sequence in j, the iteration index, of inputs $u_j(k)$ with $k \in [0, N-1]$ so that the error $e_j(k) \equiv y_d(k) - y_j(k)$ becomes small as $j \to \infty$. All disturbances, including initial conditions, acting on the system are assumed to be iteration-invariant so that $d_j(k) = d(k)$.

The time domain input-output relationship in (1) can be written equivalently as the convolution

$$y(k) = \sum_{\tau=1}^{k} p(k-\tau)u(\tau-1) + d(k)\,, \tag{2}$$

where $p(k)$ are the discrete unit impulse response of $P(q)$ and are sometimes referred to as the Markov parameters of $P(q)$. The Markov parameters can be obtained from $P(q)$ by dividing the denominator into the numerator to obtain the infinite series. Using the convolution form of the dynamics, the outputs can be stacked in a vector to create the "lifted system" representation given by

$$\underbrace{\begin{bmatrix} y_j(1) \\ y_j(2) \\ \vdots \\ y_j(N+1) \end{bmatrix}}_{\mathbf{y}_j} = \underbrace{\begin{bmatrix} p(0) & 0 & 0 & 0 \\ p(1) & p(0) & 0 & 0 \\ \vdots & \ddots & \ddots & 0 \\ p(N) & \cdots & p(1) & p(0) \end{bmatrix}}_{\mathbf{P}} \underbrace{\begin{bmatrix} u_j(0) \\ u_j(1) \\ \vdots \\ u_j(N) \end{bmatrix}}_{\mathbf{u}_j} + \underbrace{\begin{bmatrix} d(1) \\ d(2) \\ \vdots \\ d(N+1) \end{bmatrix}}_{\mathbf{d}} \tag{3}$$

where $\mathbf{d}$ is the vector of disturbances, $\mathbf{u}_j$ is the vector of ILC inputs, $\mathbf{y}_j$ is the vector of plant outputs and $\mathbf{P}$ is a lower triangular Toeplitz matrix of the plant's Markov paramters. Defining $\mathbf{y_d}$ similarly as the vector of desired outputs on $[1, N+1]$, then the error vector becomes

$$\mathbf{e}_j = \mathbf{y_d} - \mathbf{y}_j \tag{4}$$

The most common ILC learning algorithm is the first-order learning function given by

$$\mathbf{u}_{j+1} = \mathbf{Q}(\mathbf{u}_j + \mathbf{L_e}\mathbf{e}_j) \tag{5}$$

where $\mathbf{Q}$ and $\mathbf{L_e}$ are NxN. Substitution of (3) and (4) into (5) yields the iteration-to-iteration dynamics of the ILC control given by

$$\mathbf{u}_{j+1} = \mathbf{Q}(\mathbf{I} - \mathbf{L_e}\mathbf{P})\mathbf{u}_j + \mathbf{Q}\mathbf{L_e}(\mathbf{y_d} - \mathbf{d})\,. \tag{6}$$

Theorem 1: The ILC system with the plant dynamics (3) and learning function (5) is stable if and only if

$$\left|\lambda_i\left(\mathbf{Q}(\mathbf{I} - \mathbf{L_e}\mathbf{P})\right)\right| < 1 \quad \forall i\,. \tag{7}$$

where $\lambda_i(\cdot)$ is the i^{th} eigenvalue.

Proof: The term $\mathbf{Q}\mathbf{L_e}(\mathbf{y_d} - \mathbf{d})$ is constant and bounded, so $\mathbf{u}_j$ converges if and only if (7). The convergence of $\mathbf{u}_j$ implies convergence of $\mathbf{y}_j$ and $\mathbf{e}_j$ through (3) and (4). ■

In [6], it was shown that if $\mathbf{L_e}$ and $\mathbf{Q}$ are restricted to the structure

$$\mathbf{L_e} = \begin{bmatrix} l_e(0) & & & & \\ l_e(1) & l_e(0) & & 0 & \\ l_e(2) & l_e(1) & l_e(0) & & \\ \vdots & \ddots & \ddots & \ddots & \\ l_e(N) & l_e(N-1) & \cdots & l_e(1) & l_e(0) \end{bmatrix} \tag{8}$$

and

$$\mathbf{Q}=\begin{bmatrix} q_1(0) & & & & \\ q_2(1) & q_2(0) & & 0 & \\ q_3(2) & q_3(1) & q_3(0) & & \\ \vdots & \ddots & \ddots & \ddots & \\ q_N(N) & q_{N-1}(N-1) & \cdots & q_N(1) & q_N(0) \end{bmatrix} \quad (9)$$

respectively, then $\mathbf{Q(I-L_eP)}$ is lower triangular and the eigenvalue stability condition of (7) can be reduced to the scalar condition involving only the diagonal elements given by

$$\left|q_k(0)\left(1-l_e(0)p(0)\right)\right|<1 \quad \forall k\,. \quad (10)$$

The Q-filter is typically a low-pass filter with the performance/robustness tradeoff that lower bandwidth results in higher performance, but lower robustness, while higher bandwidth achieves the opposite [9,10]. In [8] it was shown that an LTV Q-filter can sometimes achieve higher levels of performance and robustness over an LTI Q-filter.

One method of constructing **Q** to behave as a time-varying filter is to partition **Q** into its N rows as indicated by the subscripts of **Q**'s elements in (9). Setting the elements of the k^{th} row to the Markov parameters for a filter having bandwidth $\Omega(k)$ (rad/s) will result in **Q** emulating a moving average filter with a time-varying bandwidth profile $\Omega(k)$. Specifically, the one-sided Gaussian filter will be used here. The Markov parameters for this filter are given by

$$q_k\left(l,\Omega(k)\right)=\begin{cases} \dfrac{\exp\left(-\dfrac{l^2T^2\Omega(k)^2}{\ln 4}\right)}{\displaystyle\sum_{i=0}^{M}\exp\left(-\dfrac{l^2T^2\Omega(k)^2}{\ln 4}\right)} & ,\ 0\le l\le M \\ 0 & ,\ \text{otherwise} \end{cases} \quad (11)$$

where $\Omega(k)$ approximates the bandwidth in rad/s, T is the sample period, and M is the FIR filter width.

For the LTV filter to achieve high levels of performance, however, it must be designed appropriately according to the plant dynamics and disturbances. An alternative approach that uses an adaptive algorithm to generate the time-varying filter bandwidth profile online was developed and presented in [5]. This algorithm only modifies the filter matrix **Q** and does not alter the learning matrix $\mathbf{L_e}$. Therefore, this adaptive algorithm is compatible with most zero error ILC designs for $\mathbf{L_e}$ that assume **Q=I**, and can be combined with these designs to enhance their robustness with minimal impact to performance.

The time-varying Q-filter adaptive algorithm was discussed in detail in [7] and is briefly presented here for completeness. The adaptive algorithm adjusts the Q-filter bandwidth through local analysis of the frequency content and magnitude of the tracking error signal. The Wigner-Ville time-frequency (*t-f*) distribution [11] is used to determine the frequency content of signal locally in time. The Wigner-Ville distribution is similar to a Short Time Fourier Transform, but can yield better resolution simultaneously in time and frequency. The discrete, truncated *t-f* distribution for a real signal is given as

$$W(k,\omega)=\frac{1}{\pi}\sum_{\tau=-N}^{N}e(k-\tau)e(k+\tau)\exp(-j2\omega\tau) \quad (12)$$

and yields an energy distribution of the signal, e, simultaneously in time, k, and frequency, ω. To estimate the frequency content of the signal, a level set offset a distance, c, parallel to the time-frequency plane is used. A bounding function, $F(k)$, is defined from the intersection of the level set and the *t-f* distribution as

$$F(k)=\begin{cases} 0 & ,\ \text{if } W(k,\omega)\ne c\ \forall\omega \\ \max\ \omega\ s.t.\ W(k,\omega)=c & ,\ \text{otherwise} \end{cases} \quad (13)$$

The bounding function provides a very useful interpretation of the frequency content of the signal and is the primary adaptation mechanism in the algorithm.

To aid in determining whether or not the adaptation is improving performance, the Short Time Error Norm (STEN), defined as

$$S(k)=\frac{1}{2N_S}\sum_{\tau=-N_S}^{N_S}e_i^2(k-\tau), \quad (14)$$

is used. The STEN will be used in the adaptation to determine if changes in the bandwidth are improving the error local to a specific time, t. The STEN will also be used to scale the bounding function so that time instants with large STEN are emphasized in the adaptation.

The adaptation algorithm is

$$\Omega_{i+1}(k)=L(q)\left[\Omega_i(k)-\text{sgn}\left[\left(\Omega_i(k)-\Omega_{i-1}(k)\right)\cdot\left(S_i(k)-S_{i-1}(k)\right)\right]\cdot F_i(i)\cdot\frac{S_i(k)}{\max_k\left(S_i(k)\right)}\right] \quad (15)$$

where $L(q)$ is a low-pass filter to smooth the bandwidth transitions. The adaptation occurs as follows. First the *t-f* function, bounding function, and STEN are calculated. Then the bandwidth is updated according to (15). Last the Q-filter matrix **Q** is updated using the bandwidth profile according to (9) and (11). The level set height, c, STEN width, N_S, and filter $L(q)$ are tunable parameters to adjust the behavior of the adaptation. The interested reader is referred to [7] for more information.

In [7] it was argued that the adaptive algorithm and update in **Q** should not be run each iteration because the adaptation dynamics may interfere with the learning dynamics. Instead, if the adaptation occurs less frequently than the learning, then the adaptation dynamics become relatively slow and the learning dynamics relatively fast. In

this sense, an "iteration-scale" separation in dynamics exists and the stability of each set of dynamics independently implies stability of the combined system. In the following section it is shown that there does exist a finite iteration-scale separation parameter that guarantees stability for the entire system. A switched systems analysis is used to prove the existence of this parameter, which, in the switched systems framework, is referred as the minimum dwell time.

III. BIBO Stability of the Adaptive Q-filter Algorithm

In this section a proof of BIBO stability for the adaptive Q-filter algorithm will be presented. The following assumptions are made.

Assumption 1: The learning matrix is of the form of (8) and chosen such that $|1-l_e(0)p(0)|<1$.

Assumption 2: The filter matrix, $\mathbf{Q}$ belongs to $\mathfrak{Q}$ where $\mathfrak{Q}$ is the set of all matrices of the structure of (9) with $q_k(l,\Omega(k))$ defined in (11) for any $\Omega(k)\in[0,\infty)$.

The first assumption is satisfied by all zero-error ILC designs assuming perfect plant knowledge. Even for highly uncertain plants, the first assumption can be satisfied if the sign and an upper bound on $p(0)$ are known through an appropriate choice of learning function. The second assumption requires that the filter type be the one-sided Gaussian structure in (11). Other causal, stable filter types could be used with minor modification to the proof.

First it is shown that the above assumptions are sufficient to guarantee stability for any fixed in iteration, time-varying filter.

Theorem 2: If Assumptions 1 and 2 are satisfied, the ILC system (3,5,9) will be stable for any time-varying filter bandwidth profile Ω(k).

Proof: By assumption 2, the 0th Markov parameter of the Gaussian filter (11) is bounded as $0<q_k(0,\Omega(k))<1$ for any bandwidth $0\le\Omega(k)<\infty$. Then, by assumption 1,

$$|q_k(0)(1-l_e(0)p(0))|\le|1-l_e(0)p(0)|<1, \text{ for all } k,$$

and therefore the scalar stability condition of (10) is satisfied. ■

The following lemma will prove the intermediate result that the sequence $\left\|\left[\mathbf{Q}(\mathbf{I}-\mathbf{L_e}\mathbf{P})\right]^j\right\|_2$ is bounded by a convergent geometric series $\bar{\kappa}\bar{\gamma}^j$ for all time-varying Q-filters. This sequence can be interpreted as the worst case convergence transients of $\mathbf{u}_j$, when the forcing term $\mathbf{y_d}$-$\mathbf{d}$ is zero and the Q-filter is not updated.

Lemma 1: Let an ILC system be described by (3,5,9) and let Assumptions 1 and 2 hold. Then for any $\mathbf{Q}\in\mathfrak{Q}$, there exists a $\bar{\gamma}\in[0,1)$ and $\bar{\kappa}\in(0,\infty)$ such that

$$\left\|\left[\mathbf{Q}(\mathbf{I}-\mathbf{L_e}\mathbf{P})\right]^j\right\|_2\le\bar{\kappa}\bar{\gamma}^j \tag{16}$$

where $\|\cdot\|_2$ is the induced 2-norm defined as $\|\mathbf{M}\|_2\equiv\bar{\sigma}(\mathbf{M})$, the maximum singular value of $\mathbf{M}$.

Proof: See Appendix.

Let the sequence of iterations that an adaptive update occurs on be given by

$$\{s_i\}=\left\{0,n_1,n_1+n_2,...,\sum_{l=0}^{i}n_l,\dots\right\}$$

with $0<n_i<\infty$. That is, $\mathbf{Q}_1$ is the filter for the first n_1 iterations, and at the s_1^{th} iteration, $\mathbf{Q}_2$ becomes the filter. $\mathbf{Q}_2$ is the filter for the next n_2 iterations until the s_2^{th} iteration, and so on. Then the $\mathbf{u}_j$ dynamics in (6) can be written as

$$\mathbf{u}_j=\left[\mathbf{Q}_i(\mathbf{I}-\mathbf{L_e}\mathbf{P})\right]^{j-s_i}\mathbf{u}_{s_i}+\sum_{l=0}^{j-s_i-1}\left[\mathbf{Q}_i(\mathbf{I}-\mathbf{L_e}\mathbf{P})\right]^l\mathbf{Q}_i\mathbf{L_e}(\mathbf{y_d}-\mathbf{d}) \tag{17}$$

for $s_i+1\le j\le s_{i+1}-1$ and

$$\mathbf{u}_{s_{i+1}}=\left[\mathbf{Q}_{i+1}(\mathbf{I}-\mathbf{L_e}\mathbf{P})\right]^{n_i}\mathbf{u}_{s_i}+\sum_{l=0}^{n_i-1}\left[\mathbf{Q}_{i+1}(\mathbf{I}-\mathbf{L_e}\mathbf{P})\right]^l\mathbf{Q}_{i+1}\mathbf{L_e}(\mathbf{y_d}-\mathbf{d}) \tag{18}$$

for $j=s_i$. The following theorem presents the central result of this paper which is stability for the adaptive Q-filter algorithm given a sufficiently large dwell time.

Theorem 3: Let an ILC system be described by (3,5,9). If Assumptions 1 and 2 are satisfied, then there exists $\bar{n}$ such that the adaptive Q-filter ILC system is BIBO stable for any update sequence $\{s_i\}$ with $n_i\ge\bar{n}$ for all $i=1,2,\dots$.

Proof: First, $\mathbf{u}_j$ will be shown to be bounded during the period between updates for $s_i+1\le j\le s_{i+1}-1$. From Lemma 1, $\left\|\left[\mathbf{Q}(\mathbf{I}-\mathbf{L_e}\mathbf{P})\right]^j\right\|_2\le\bar{\kappa}\bar{\gamma}^j$, so (16) becomes

$$\|\mathbf{u}_j\|_2\le\bar{\kappa}\bar{\gamma}^{j-s_i}\|\mathbf{u}_{s_i}\|_2+\sum_{l=0}^{j-s_i-1}\bar{\kappa}\bar{\gamma}^l\|\mathbf{Q}_i\|_2\|\mathbf{L_e}(\mathbf{y_d}-\mathbf{d})\|_2. \tag{19}$$

Then $\|\mathbf{Q}_i\|_2\le\sqrt{N}\|\mathbf{Q}_i\|_\infty\le\sqrt{N}$ because each row sum of $\mathbf{Q}_i$ is the sum of the Markov parameters in (11) for a particular bandwidth which sums to 1. Then, (19) can be further simplified as

$$\left\|\mathbf{u}_j\right\|_2 \le \bar{\kappa}\left\|\mathbf{u}_{s_i}\right\|_2 + \underbrace{\frac{\bar{\kappa}}{1-\bar{\gamma}}\sqrt{N}\left\|\mathbf{L_e}\left(\mathbf{y_d}-\mathbf{d}\right)\right\|_2}_{\text{constant}}. \qquad (20)$$

Then $\left\|\mathbf{u}_j\right\|_2$ is bounded for $s_i+1 \le j \le s_{i+1}-1$, if $\left\|\mathbf{u}_{s_i}\right\|_2$ is bounded. All that remains is to show that the sequence $\mathbf{u}_{s_i}$ remains bounded. The sequence in (18) can be bounded similarly as

$$\left\|\mathbf{u}_{s_{i+1}}\right\|_2 \le \bar{\kappa}\bar{\gamma}^{n_i}\left\|\mathbf{u}_{s_i}\right\|_2 + \frac{\bar{\kappa}}{1-\bar{\gamma}}\sqrt{N}\left\|\mathbf{L_e}\left(\mathbf{y_d}-\mathbf{d}\right)\right\|_2. \qquad (21)$$

Let $\bar{n} > \dfrac{\log 1/\bar{\kappa}}{\log \bar{\gamma}}$. Then if $n_i \ge \bar{n}$,

$$\left\|\mathbf{u}_{s_{i+1}}\right\|_2 < \left\|\mathbf{u}_{s_i}\right\|_2 + \frac{\bar{\kappa}}{1-\bar{\gamma}}\sqrt{N}\left\|\mathbf{L_e}\left(\mathbf{y_d}-\mathbf{d}\right)\right\|_2 \qquad (22)$$

and the sequence $\left\|\mathbf{u}_{s_i}\right\|_2$ is bounded. ■

The above theorem shows that there exists a minimum dwell time, $\bar{n}$, previously referred to as the iteration-scale separation parameter in [5], that will guarantee stability of the adaptive Q-filter method. However, actually finding the minimum dwell time requires that a $\bar{\kappa}$ and $\bar{\gamma}$ be found. Solving for a κ_i and γ_i for a specific $\mathbf{Q}_i$ is straightforward (see the proof to Lemma 1 in the Appendix), but solving for $\bar{\kappa}$ and $\bar{\gamma}$ requires solving for the set of solutions to the Lyapunov equation which corresponds to the full set of possible filter matrices $\mathbf{Q}$. In general, this may be a difficult problem. Further, the minimum dwell time may be impractically large. However, the above solution provides a framework for stability and demonstrates that the adaptive Q-filter approach can be made stable independent of the algorithm used to generate the filter matrices $\mathbf{Q}_i$. By restricting the filter set and incorporating knowledge of the adaptive algorithm, small dwell times may be possible.

IV. Tracking and Manufacturing Results

The adaptive Q-filter algorithm in (20) is applied to the ILC for position control of the X and Y axes on the μ-RD machine discussed in Section I. The learning function for each axis is the basic PD-type. The learning gains and adaptive algorithm parameters were tuned to achieve good learning and adaptation transients. These parameter values are identical to those used in [7]. A 3-D reference trajectory shown in Figure 3 is used to test the performance of the algorithm. An iteration-scale separation factor of $\bar{n}=15$ is used. The results using this separation factor are sufficient to observe stable behavior of the adaptive algorithm. The converged error is shown by the shading of the trajectory of Figure 3 with the largest contour errors on the trajectory less than 10 μm.

Figure 4 shows the max and RMS norms of the error signal against the iteration index for the X and Y axes. The Q-filter switches are marked every 15 iterations with vertical lines. Before the first switch there is a large decrease in error corresponding to the dominantly low frequency error that can be learned and removed with the initial low bandwidth Q-filter. To decrease the error below this initial level, the adaptive algorithm increases the bandwidth for short periods around the many acceleration and deceleration points in the reference trajectory. When changes are too large, small increases in error occur and the algorithm reduces the bandwidth on the following update to compensate.

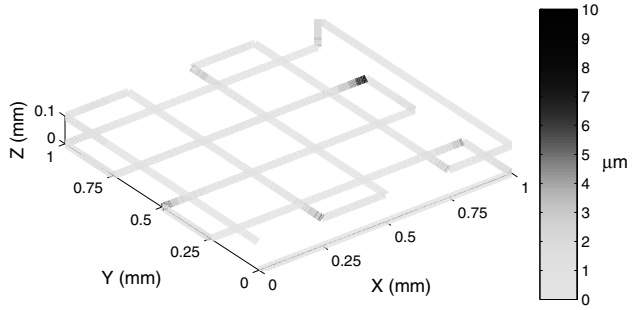

Fig. 3. Converged contour error for the causal Q-filter adaptive algorithm.

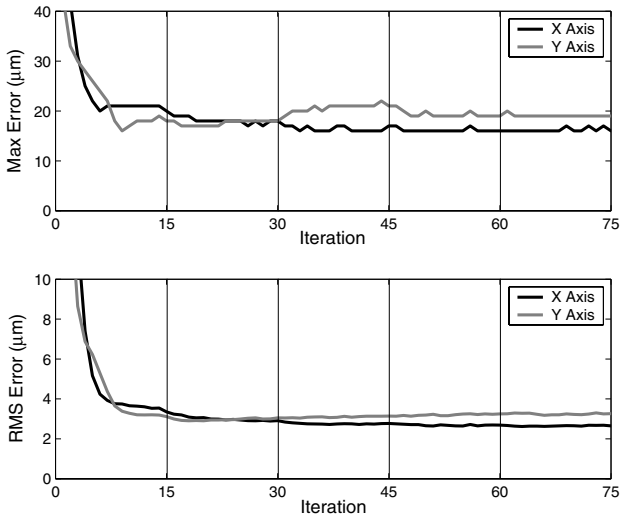

Fig. 4. Convergence RMS and Max error profiles for the causal Q-filter adaptive algorithm.

The performance demonstrated by the adaptive algorithm with the causal filter in Figures 3 and 4, however, are lower than the results reported in [7] for the adaptive algorithm with a non-causal filter, two-sided Gaussian filter. These results are repeated in Figures 5 and 6 for comparison and summarized in Table 1 which shows that non-causal filtering yields approximately 75% improvement over the casual filtering in each category. The stability proof in Section III will be expanded in future work to capture the

benefits of non-causal filtering that are demonstrated in Table1.

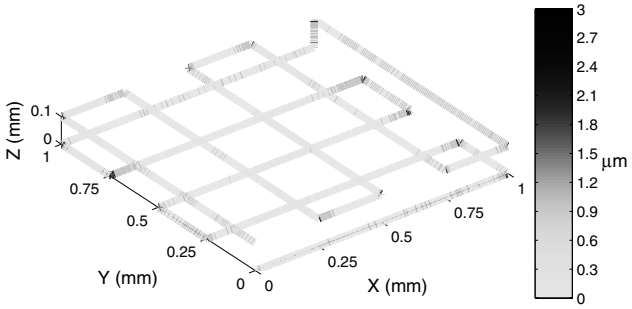

Fig. 5. Converged contour error for the *non-causal* Q-filter adaptive algorithm.

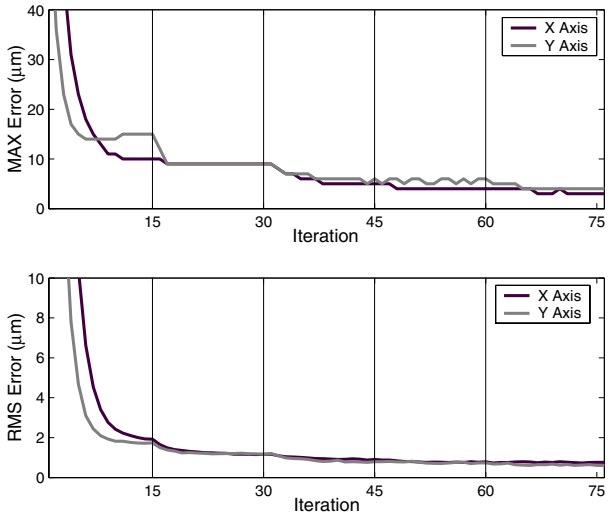

Fig. 6. Convergence RMS and Max error profiles for the *non-causal* Q-filter adaptive algorithm.

Table 1. Comparison of tracking performance for causal and non-causal Q-filtering.

	X		Y		Contour
	Max (µm)	RMS (µm)	Max (µm)	RMS (µm)	Error (µm)
Initial Error without ILC	117	63.62	69	48.73	110
Causal Q	16	2.65	19	3.26	10
Non-Causal Q	3	0.76	4	0.60	3

The low contour error achieved by the adaptive algorithm with the causal filtering indicates that performance is sufficient for deposition of parts with feature sizes larger than 30 µm. For smaller feature sizes, the non-causal filtering may be necessary. However, to demonstrate the capabilities of the prototype two-ink valve, a mesoscale feature sized part is constructed. Future versions of the two-ink valve capable of constructing microscale feature sizes are currently being developed. The part design [4] is the University of Illinois Illini logo using a 0.6 mm deposition nozzle. The part is constructed using an orange and a blue dyed ink and shown in Figure 7.

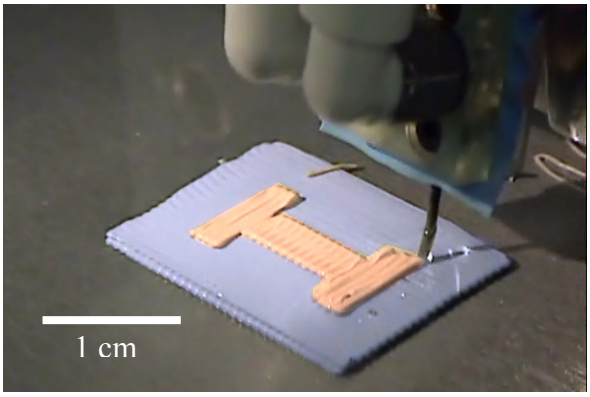

Fig. 7. Two-ink Illni logo.

V. Conclusions

In this paper the µ-RD manufacturing technique was discussed and precision motion control was identified as a key factor in part quality. To provide precise motion control, an adaptive ILC strategy using a time-varying Q-filter was adopted. A key result presented in this paper is the existence of a dwell time for which the adaptive algorithm using a causal Q-filter is BIBO stable.

The adaptive Q-filtered ILC algorithm was applied to the motion control of each axis of the µ-RD machine. Experimental results for a sample 3-D trajectory demonstrated the ability of the adaptive algorithm to improve performance while maintaining stability and avoiding large transients. Results for the adaptive algorithm using a non-causal Q-filter were presented for comparison and demonstrated that non-causal Q-filtering can lead to improved performance. Future work will involve expansion of the stability proof in Section III to capture the benefits of non-causal filtering.

Appendix

Proof of Lemma 1: First it will be shown that for any $\mathbf{Q} \in \mathfrak{Q}$, the sequence $\left\|\left[\mathbf{Q}\left(\mathbf{I}-\mathbf{L}_e\mathbf{P}\right)\right]^j\right\|_2 \le \kappa\gamma^j$ for some κ, γ associated with the specific $\mathbf{Q}$. Then it will be shown that there is a $\bar{\kappa} \ge \kappa$ and $\bar{\gamma} \ge \gamma$ for all such κ, γ.

Let $\mathbf{x}_{j+1} = \mathbf{Q}\left(\mathbf{I}-\mathbf{L}_e\mathbf{P}\right)\mathbf{x}_j$. Then from Theorem 2 it is true that $\left|\lambda_i\left(\mathbf{Q}\left(\mathbf{I}-\mathbf{L}_e\mathbf{P}\right)\right)\right| < 1$ for all i. Therefore, there exists an $\mathbf{M} = \mathbf{M}^T > 0$ that is the solution to the Lyapunov equation

$$\left(\mathbf{I}-\mathbf{L}_e\mathbf{P}\right)^T\mathbf{Q}^T\mathbf{M}\mathbf{Q}\left(\mathbf{I}-\mathbf{L}_e\mathbf{P}\right)-\mathbf{M} = -\eta\mathbf{I} \qquad (23)$$

for some η>0. Let $\mathbf{V}_j = \mathbf{x}_j^T\mathbf{M}\mathbf{x}_j \ge 0$ be the Lyapunov function candidate. Then

$$\mathbf{V}_{j+1} - \mathbf{V}_j = -\eta \mathbf{x}_j^T \mathbf{x}_j \le 0 . \quad (24)$$

Using (28) and the relationship from [12] that

$$\lambda_{\min}(\mathbf{M}) \mathbf{x}_j^T \mathbf{x}_j \le \mathbf{V}_j \le \lambda_{\max}(\mathbf{M}) \mathbf{x}_j^T \mathbf{x}_j , \quad (25)$$

then,

$$\mathbf{V}_j \le \gamma^{2j} \mathbf{V}_0 \quad (26)$$

where

$$\gamma = \left(\frac{\lambda_{\max}(\mathbf{M}) - \eta}{\lambda_{\max}(\mathbf{M})} \right)^{1/2} . \quad (27)$$

To show $0 \le \gamma < 1$, note that

$$(\mathbf{I} - \mathbf{L}_\mathbf{e}\mathbf{P})^T \mathbf{Q}^T \mathbf{M} \mathbf{Q} (\mathbf{I} - \mathbf{L}_\mathbf{e}\mathbf{P}) \ge 0 .$$

Therefore, from (22), $\mathbf{M} - \eta \mathbf{I} \ge 0$ which implies that $\lambda_{\max}(\mathbf{M}) - \eta \ge 0$. From (24) and (25),

$$\left\| \mathbf{x}_k \right\|_2 \le \gamma^k \kappa \left\| \mathbf{x}_0 \right\|_2 \quad (28)$$

where

$$\kappa = \left(\frac{\lambda_{\max}(\mathbf{M})}{\lambda_{\min}(\mathbf{M})} \right)^{1/2} \quad (29)$$

and $0 < \kappa < \infty$ because **M**>0. Finally, by definition,

$$\left\| \left[\mathbf{Q}(\mathbf{I} - \mathbf{L}_\mathbf{e}\mathbf{P}) \right]^j \right\|_2 = \sup_{\mathbf{x_0}} \frac{\left\| \left[\mathbf{Q}(\mathbf{I} - \mathbf{L}_\mathbf{e}\mathbf{P}) \right]^j \mathbf{x_0} \right\|_2}{\left\| \mathbf{x_0} \right\|_2} = \sup_{\mathbf{x_0}} \frac{\left\| \mathbf{x}_j \right\|_2}{\left\| \mathbf{x_0} \right\|_2} \le \gamma^j \kappa , \quad (30)$$

thus completing the first part of the proof. To show the second part of the proof that there is a bounded $\bar{\kappa}$ and $\bar{\gamma}$ which are larger than all κ and γ, define the set $\bar{\mathfrak{Q}} \subset R^{NxN}$ as

$$\bar{\mathfrak{Q}} \equiv \left\{ \mathbf{Q} \in R^{NxN} : \mathbf{Q} = \begin{bmatrix} q_{1,1} & & 0 \\ \vdots & \ddots & \\ q_{N,1} & \cdots & q_{N,N} \end{bmatrix} s.t. \; 0 \le q_{i,j} \le 1 \right\} . \quad (31)$$

Then $\mathfrak{Q} \subset \bar{\mathfrak{Q}}$ because $0 \le q_k(l, \Omega(k)) \le 1$ for the one-sided Gaussian filter. Because $q_{i,i}$<1, Assumption 1 implies that all $\mathbf{Q} \in \bar{\mathfrak{Q}}$ stabilize the ILC system. Then, for each $\mathbf{Q} \in \bar{\mathfrak{Q}}$ there is an **M** that satisfies (22). But, $\bar{\mathfrak{Q}}$ is a closed bounded set, so there exists a closed bounded set $\mathcal{M}$ of solutions **M** in (22) corresponding to the set $\bar{\mathfrak{Q}}$ for a fixed $\hat{\eta}$. Because $\mathcal{M}$ is closed and bounded, there exists $\bar{\mathbf{M}}, \underline{\mathbf{M}} \in \mathcal{M}$ such that $\lambda_{\max}(\bar{\mathbf{M}}) \ge \lambda_{\max}(\mathbf{M})$ and $\lambda_{\min}(\underline{\mathbf{M}}) \ge \lambda_{\max}(\mathbf{M})$ for all $\mathbf{M} \in \mathcal{M}$. Then for any $\mathbf{Q} \in \bar{\mathfrak{Q}}$

$$\left\| \left[\mathbf{Q}(\mathbf{I} - \mathbf{L}_\mathbf{e}\mathbf{P}) \right]^j \right\|_{i2} \le \bar{\kappa} \bar{\gamma}^j \quad (32)$$

where

$$\bar{\gamma} = \left(\frac{\lambda_{\max}(\bar{\mathbf{M}}) - \hat{\eta}}{\lambda_{\max}(\bar{\mathbf{M}})} \right)^{1/2}$$

$$\bar{\kappa} = \left(\frac{\lambda_{\max}(\bar{\mathbf{M}})}{\lambda_{\min}(\underline{\mathbf{M}})} \right)^{1/2} \quad (33)$$

which completes the proof. ■

ACKNOWLEDGMENTS

The authors would like to express their gratitude to Marina Tharayil for insightful discussions on time-varying Q-filtering and switched systems analysis.

REFERENCES

[1] Bristow, D. and A. Alleyne, "A Manufacturing System for Microscale Robotic Deposition", *Proceedings of the American Controls Conference*, pp.2620-2625, 2003.

[2] Cesarano, J., R. Segalman, and P. Calvert, "Robocasting Provides Moldless Fabrication from Slurry Deposition", *Ceramic Industry*, pp. 94-102, 1998.

[3] Li, Q. and J. Lewis, "Nanoparticle Inks for Directed Assembly of Three-Dimensional Periodic Structures", *Advanced Materials*, vol. 15, no. 19, pp. 1639-1643, Oct 2003.

[4] Alleyne, A., P. Ferreira, D. Bristow, D. Mukhopadhyay, J. Lewis, and G. Gratson, "Process Planning and a New Dual-Ink Write Head for Microscale Robotic Deposition", *NSF Design, Service and Manufacturing Research and Grantees Conference*, Scottsdale, Arizona, Jan. 2005.

[5] Moore, K.L., *Iterative Learning Control for Deterministic Systems*, Germany: Springer-Verlag, 1993.

[6] Xu, J.-X. and Y. Tan, *Linear and Nonlinear Iterative Learning Control*, Berlin: Springer, 2003.

[7] Bristow, D., A. Alleyne, and D. Zheng, "Control of a Microscale Deposition Robot Using a New Adaptive Time-Frequency Filtered Iterative Learning Control", *Proceedings of the American Controls Conference*, 2004.

[8] Tharayil, M. and A. Alleyne, "A Time-Varying Iterative Learning Control Scheme", *Proceedings of the American Controls Conference*, 2004.

[9] Kavli, T., "Frequency Domain Synthesis of Trajectory Learning Controllers for Robot Manipulators", *Journal of Robotic Systems*, Vol. 9, No. 5, pp. 663-680, 1992.

[10] de Roover, D. and O.H. Bosgra, "Synthesis of Robust Multivariable Iterative Learning Controllers with Application to a Wafer Stage Motion System," *International Journal of Control*, Vol. 73, No. 10, pp. 968-979, 2000.

[11] Cohen, L., *Time-Frequency Analysis*, NJ: Prentice Hall, 1995.

[12] Liberzon, D., *Switching in Systems and Control,* Boston: Birkhäuser, 2003.